Green Synthesis of ZnO NPs Using Extract of *Zingiber Officinale* Root and Garlic Bulb (*Allium Sativum*) and their Antibacterial Activities

Solomon Kebede Urge

A Thesis Submitted to the Department of Applied Physics

School of Applied Natural Science

Presented in Partial Fulfillment of the Requirement for the Degree of Master's in Applied Physics (Material Physics)

Office of Graduate Studies

Adama Science and Technology University

June 10, 2022

Adama, Ethiopia

Green Synthesis of ZnO NPs Using Extract of *Zingiber Officinale* Root and Garlic Bulb (*Allium Sativum*) and their Antibacterial Activities

Solomon Kebede Urge

Advisor

Solomon Tirunah Dibaba (PhD)

Co-Advisor

Ababa Belay Gemta (PhD)

A Thesis Submitted to the Department of Applied Physics

School of Applied Natural Science

Presented in Partial Fulfillment of the Requirement for the Degree of Master's in Applied Physics (Material Physics)

Office of Graduate Studies

Adama Science and Technology University

June 10, 2022

Adama, Ethiopia

Declaration

I hereby declare that this Master Thesis entitled "**Green Synthesis of ZnO NPs using *Z.officinale* root extract and Garlic Bulb extract and their Antibacterial activities**" is my original work. That is, it has not been submitted for the award of any academic degree, diploma or certificate in any other university. All sources of materials that are used for this thesis have been duly acknowledged through citation.

_____	_____	_____
Name of the student	Signature	Date

Recommendation

I/we, the advisor(s) of this thesis, hereby certify that I/we have read the revised version of the thesis entitled "**Green Synthesis of ZnO NPs using *Z.officinale* root extract and Garlic Bulb extract and their Antibacterial activities** prepared under my/our guidance by **Selemon Kebede Urge** submitted in partial fulfillment of the requirements for the degree of Masters of Science in Applied Physics (Materials Physics). Therefore, I/we recommend the submission of revised version of the thesis to the department following the applicable procedures.

_____	_____	_____
Major Advisor	Signature	Date
_____	_____	_____
Co-advisor	Signature	Date

APPROVAL PAGE

I/we, the advisors of the thesis entitled "**Green Synthesis of ZnO NPs using *Z.officinale* root extract and Garlic Bulb extract and their Antibacterial activities**" and developed by **Selemon Kebede Urge** hereby certify that the recommendation and suggestions made by the board of examiners are appropriately incorporated into the final version of the thesis.

_____	_____	_____
Major Advisor	Signature	Date
_____	_____	_____
Co-advisor	Signature	Date

We, the undersigned, members of the Board of Examiners of the thesis by **Selemon Kebede Urge** have read and evaluated the thesis entitled "**Green Synthesis of ZnO NPs using *Z.officinale* root extract and Garlic Bulb extract and their Antibacterial activities** and examined the candidate during open defense. This is, therefore, to certify that the thesis is accepted for partial fulfillment of the requirement of the degree of Master of Science in Applied Physics (Materials Physics).

Chairpersons	Signature	Date
_____	_____	_____
Internal Examiner	Signature	Date
_____	_____	_____
External Examiner	Signature	Date
_____	_____	_____

Final approval and acceptance of the thesis is contingent upon submission of its final copy to the Office of Postgraduate Studies (OPGS) through the Department Graduate Council (DGC) and School Graduate Committee (SGC).

Department Head	Signature	Date
_____	_____	_____
School Dean	Signature	Date
_____	_____	_____
Office of Postgraduate Studies, Dean	Signature	Date
_____	_____	_____

AKNOWLEDGEMENT

First of all, I would like to thanks Almighty **God who** can protect me all the time without interruption of a second. Secondly, I would like to thanks Adama Science and Technology University, School of Applied Natural Science, Applied Physics Department for their good support of the money and materials needed for my **Thesis**. Then, I would like to thanks my Advisor **Solomon Tiruneh Dibaba (PhD)**, he can sacrifices his time to advise me in order to get the good result of experiment as much as possible and Co-advisor **Abebe Belay Gemta (PhD),** he also sacrifices his time to advise me and supported me within the chemicals needed for my work. I would glad to School of Materials Engineering for their good support of materials needed for characterization (XRD and UV-vis Spectroscopy) and their Lab Technician Mr. Demeke who was done XRD and UV-vis Spectroscopy characterization of my sample. Finally I would like to thanks all my friends, Advisor and Co-advisor for they shared me a good idea to succeed in my work.

CONTENTS

CHAPTER **PAGE**

LIST OF TABLES

TABLE **PAGE**

LIST OF FIGURES

FIGURE **PAGE**

Acronyms

AATC……...American Type Culture Collection

AgO……..Silver Oxide

CFU……..Colony Forming Unit

CVD …….....Chemical Vapor Deposition

FTIR …….Fourier Transform Infra-Red

G-ve……...Gram Negative

G+ve……..Gram Positive

MHA…….Muller Hilton Agar

MIC ……..……Minimum Inhibitory Concentration

MONPs…….Metal Oxide Nanoparticles

NPs…….……...Nano Particles

PL …….Photo Luminescence

TiO_2……..Titanium Oxide

UV-Vis …….Ultraviolet-Visible

XRD …….X-ray Diffraction

ZnO ……...Zinc Oxide

Abstract

*In this paper, ZnO NPs were synthesized through green method using Garlic Bulb (Allium Sativum) extract, Zingiber officinale (Ginger) root extract and their mixture. The synthesized ZnO NPs were characterized through XRD, UV-Vis, PL spectroscopy and FTIR spectroscopy. The functional group of synthesized ZnO NPs was characterized using FTIR spectroscopy. The crystalline sizes and peak absorbance of ZnO NPs synthesized using Garlic Bulb (Allium Sativum) extract; Zingiber officinale (Ginger) root extract and their mixture were found to be 19.8 nm, 21.94 nm, 23.86 nm and 369.5 nm, 377.5 nm and 374 nm with band gap of 3.375 eV, 3.3 eV, 3.325 eV respectively. The antimicrobial activities of synthesized ZnO NPs were tested against Gram Negative bacteria (E.coli and P.putida) and Gram Positive bacteria (S.aureus and S.pyogenes). According to the recorded data ZnO NPs synthesized using the mixture of Garlic Bulb (Allium Sativum) and Z.officinale (Ginger) root extract was shown maximum inhibition zone against G-ve bacteria P.putida (28.67± 0.82 mm) and G+ve bacteria S.aureus (15.67±0.47 mm) respectively. ZnO NPs mediated Garlic Bulb and Z.officinale root extract were indicated maximum inhibition zone against G-ve bacteria E.coli (*19±0.82 mm*) and G+ve bacteria S.aureus (16.4± 0.47mm) respectively.*

***Key words**: Metal oxide, Green Synthesis, Precipitation, Reducing agent, Antibacterial.*

CHAPTER 1 INTRODUCTION

1.1 Background

Nanotechnologies are the design, characterisation, production and application of structures, devices and systems by controlling shape and size at nanometre scale characterized by the size 1-100 nm. These are actually modified form of basic elements derived by altering their atomic as well as molecular properties of elements (Daniel & Astruc, 2004; Kato, 2011). Nanoparticles gained considerable attraction because of their various applications, over their bulk counterparts.

MONPs are among the widest used manufactured nanomaterial because of their unique properties such as their various nonlinear optical properties, higher ductility at elevated temperatures, cold welding properties, super-paramagnetic behavior, unique catalytic, sensitivity, and selective activity (Chavali & Nikolova, 2019), magnetic, and electrical properties (Singhal & Bhavesh, 2011; Vidya et al., 2013). Among other metal NPs, ZnO NPs considered as multi task Metal Oxide, used as Nano scale due to its unique physical, chemical and biological properties (Salam & Sivaraj, 2014). ZnO NPs has many applications in different fields: like, optical, piezoelectric, mechanical, thermodynamic, electrodynamics, electromagnetic and gas sensing (Kołodziejczak-radzimska & Jesionowski, 2014).

There are different methods of synthesizing ZnO NPs, including thermal evaporation, organometallic synthesis, Sol-gel processing, homogeneous precipitation, microwave methods and green synthesis. Among these synthesis methods, green synthesis using plant extracts are commonly preferred for the synthesis of ZnO NPs due to eco-friendly, cost effective, save nature of the resulting NPs for the human therapeutic use (Dönmez, 2020). H. Mofid et.al (2020) synthesized ZnO NPs by using Aloe Vera plant extract for investigation of antimicrobial properties (Mofid et al., 2020). According to their report, Zone of inhibition of synthesized ZnO NPs was found to be 16 mm against E.coli for the concentration of 25 mg/mL. From the given data of present study, Zone of inhibition of ZnO NPs synthesized using the mixture of *Z.officinale* (Ginger) root and Garlic Bulb (*Allium Sativum*) extract against E.coli and P.putida were found to be 19 ± 0.82 mm and 28.67 ± 0.82 mm for the concentration of 15 mg/mL respectively. This shows good result compared to the previous work.

Ginger is the most frequently and heavily consumed dietary condiments in the world. Ginger is frequently prescribed by Indian and Chinese medicine for the treatment of cough, common cold, rheumatism, snake bite and respiratory problems (Song et al., 2006). It is also used in treatment of cancer, treating skin diseases, heart palpitation, swelling, urinary problems, stomach problems, abdomen problems, dyspsia and loss of appetite. Chemically, ginger is rich in flavonoids and polyphenolic compounds such as gingerols, shagols, zingerone, paradol, terphineol, terpenes, borneol, geraniol, limonene, linalool, alpha-zingiberene etc (Mahboubi, 2019).

Similarly, garlic is used worldwide as a food additive, spice and medicine. It has been described as a gastric stimulant. It aids digestion and is given in flatulence. It has special influence over the bronchial and pulmonary secretions and in promotion of flow of menses. Garlic is used as tonic dyspepsia, treatment of tuberculosis and stimulant, carminative, and a remedy to bites of venomous reptiles. In large doses, it is an irritant and produces flatulence, headache, nausea and even diarrhea. As a local stimulant and irritant, it causes redness of the skin. It is applied to the nose of hysterical patients when in a state of swooning and it relieves colic pain, earache, nervous headache and expels roundworms.

Garlic is a rich source of organosulphur compounds showing a variety of biological activities. The chemical constituents from garlic cloves (bulbs) vary with the isolation procedure and obviously many of the compounds reported from this source have been proved to be artifacts. Thus, while garlic oil obtained by steam distillation of garlic cloves was proved to be essentially diallyl disulphide accompanied by lesser amounts of diallyl tri-and tetra-sulphides (Singh et al., 2001).

Hence the present study undertaken in order to evaluate the efficiency of *Zingiber officinale* and Garlic Bulb (*Allium Sativum*) for the biogenic synthesized of ZnO nanoparticle.

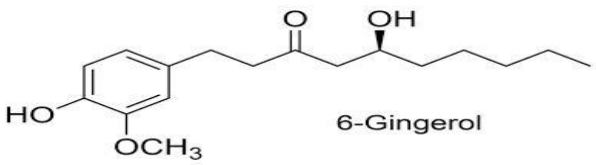

Figure 1: Chemical structures of Zingiber officinale (Ginger) (Pournaderi et al., 2017)

1.2 Statement of the Problem

The previous work on the green synthesis of ZnO NPs was not well defined the comparison of ZnO NPs synthesized from *Z.officinale* root extract, *Allium sativum* extract and their mixture. The synergetic effects of the two were not done before. In this work we could compare the role of ZnO NPs synthesized using *Z.officinale* root extract, *Allium sativum* extract and their mixture against the two standard pathogens, Gram positive and Gram negative bacteria.

1.3 Significance of the Study

The conventional chemical methods are expensive and require the use of chemical compounds and organic solvents as reducing agents; they are toxic to both human and animal. Green Synthesis shows better advantage over chemical and physical as it is lesser toxic, cost effective, environmental friendly, and also involves proteins as capping agent. In addition, Green chemistry reduces pollution risk at source level and it is enhanced to prevent waste. Because of the effectiveness of green synthesis, we could synthesize ZnO NPs by using *Z.officinale* root extract, *Allium sativum* extract and their mixture. Both ginger and garlic are used for the treatment of various diseases. This may increase the medicinal efficiency of ZnO NPs synthesized using *Z.officinale* root extract, *Allium sativum* extract and their mixture.

1.4 Objectives of the Study

1.4.1 General Objectives

The general objective of the study is to synthesize, characterize and apply ZnO Nano particle for antibacterial activities using *Zingiber officinale* (Ginger) root, Garlic Bulb (*Allium Sativum*) extract and their mixture.

1.4.2 Specific Objective

The specific objective of the study includes:

- ✓ To synthesize ZnO NPs using *Zingiber officinale* (Ginger) root extract, Garlic Bulb (*Allium Sativum*) extract and their mixture.
- ✓ To apply the synthesized ZnO NPs on antibacterial activities against Gram Negative bacteria (E. Coli and P.putida) and Gram Positive bacteria (S. Aureus and S.pyogenes).
- ✓ To compare the efficiency of antimicrobial activities of ZnO NPs synthesized using extract of Garlic Bulb (*Allium sativum*), *Zingiber offocinale* root and their mixture.

CHAPTER 2 LITERATURE REVIEW

2.1 Metal Oxide NPs

Potential technological applications of metal oxide nanoparticles attracting researchers with considerable interest from the fields of materials chemistry, medicine, agriculture, information technology, biomedical, optical, electronics, catalysis, environment, energy, and sense. Changes in cell parameters due to the size-related structural alterations have been observed, for example, in metal oxides nanoparticles of CuO, ZnO, SnO2, Al_2O_3, MgO, ZrO_2, AgO, TiO_2, CeO_2, etc. As the size decreases in the nanoparticles, an increasing number of surface and interface atoms generate strain or stress and adjoining structural perturbations (Bansal et al., 2006). The specific size of the nanoparticle can alter magnetic, conducting, chemical, and electronic properties (Liu, 2006). Magnetic, electronic, and chemical properties of nanoparticles can be dependent on a specific size of the nanoparticle material (Poole & Owens, 2003).

Electrical properties (conductance) are strongly dependent on the size of these particles especially using oxides like SnO_2, TiO_2, WO_3, and In_2O_3 in gas sensing applications(Franke et al., 2006). Electrical/ionic conductivity is a property of TiO_2 materials that modulates to find practicality in the area of sensors, optoelectronics, or photovoltaic. TiO_2 can be easily reduced at high temperatures, and this assertively impacts conductivity.

There are different types of metal oxide nanoparticles synthesized from different plant species, including, ZnO NPs, Silver Oxide NPs (AgO NPs), Nickel Oxide NPs (NiO NPs), Copper Oxide NPs, Gold NPs etc. Among all metal oxide NPs, ZnO nanoparticles have gained considerable attention for the fabrication of efficient amperometric biosensors due to their unique features that include high catalytic efficiency, high isoelectric point, nontoxicity, biocompatibility, excellent electron transfer capability, and good stability, generally recognized as safe, and exhibits antimicrobial properties(Muthuchamy et al., 2018).

2.1.1 Zinc oxide Nanoparticle (ZnO NPs)

Zinc oxide is an inorganic compound with the molecular formula ZnO. It appears as a white powder nearly insoluble in water, widely used as an additive in various materials and products including ceramics, glass, cement, rubber (e.g., car tires), lubricants, paints, ointments, adhesives, plastics, sealants, pigments, foods (source of Zn nutrient), batteries, ferrites, and fire

retardants. In the Earth crust ZnO is present as zincite mineral but mostly ZnO used for commercial purposes is produced synthetically. ZnO semiconductor has several unique properties such as good transparency, high electron mobility, wide band gap (3.3eV at room temperature), and strong room temperature luminescence. The wide band gap and large excitonic binding energy have made zinc oxide important both for scientific and industrial applications (Wang et al., 2004).

2.1.2 The properties of ZnO Nanoparticles

The crystal structure of ZnO NPs

Zinc oxide has three crystal structures such as hexagonal wurtzite, cubic zinc blend and cubic rock salt. Among these, wurtzite crystalline structure is the most stable phase at ambient conditions. In this structure every zinc atom is tetrahedral coordinated with four oxygen atoms. It has lattice parameters, a = 0.32495 nm and c = 0.52069 nm, ratio of c / a =1.6023, which is similar to the ideal value of hexagonal cell c/a = $\sqrt{\frac{8}{3}}$ = 1.633. It belongs to the space group of P63mc and is characterized by two interconnecting sub lattices of Zn^{2+} and O^{2-}. The zinc-blende structure can be achieved only by growth on cubic substrates, and the cubic rock salt is observed only at relatively high pressures ~10 GPa. The tetrahedral symmetry of wurtzite structure makes an imperative role for the polarity of ZnO that arises along the hexagonal axis. Since ZnO has sensitive lattice constants to the presence of structural point defects (oxygen vacancies and interstitial Zn ions act as donors in its lattice) and extended defects (threading/planar dislocations), it has an n-type nature.

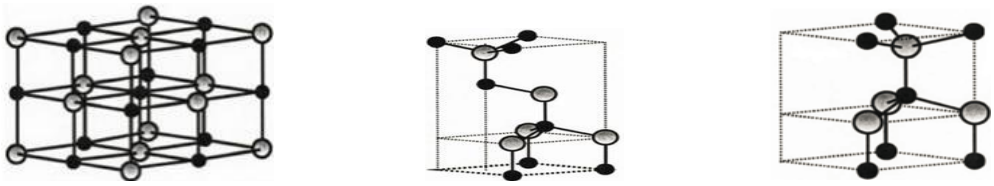

(a) ROCK SALT (b) ZINC BLEND (c) WURTZITE

Figure 2: Ball and stick representation of ZnO crystal structures: (a) cubic rock salt, (b) cubic zinc blende, (c) hexagonal wurtzite. The shade gray and black spheres denote Zn and O atoms, respectively (Cerrato et al., 2018).

The crystal structure will be investigated by XRD (x-ray diffraction) which is based on Wulf-Bragg‟s law presented in Eq (2.1).

$$n\lambda = 2d\sin\theta \tag{2.1}$$

Where n is the order of the diffraction (usually n = 1), λ is the wavelength of the X-ray radiation and d is the spacing between the planes of given Miller indices h, k and l. In the ZnO hexagonal structure, the plane spacing d is related to the lattice constants, c and the Miller indices (hkl) by the following relation.

$$d_{hkl} = \frac{ac}{2}\sqrt{\frac{3}{c^2(h^2+hk+k^2)+3\frac{(al)^2}{4}}} \tag{2.2}$$

For n=1 the Eq (2.2) can be expressed as Eq (2.3) under small angle approximation

$$sin^2\theta = \frac{\lambda^2}{4a^2}\left[\frac{4}{3}(h^2 + K^2 + hk) + \left(\frac{a}{c}\right)^2 l^2\right] \tag{2.3}$$

For (100) plane, Eq (2.3) reduced to

$$a = \frac{\lambda}{\sqrt{3}sin\theta} \tag{2.4}$$

Similarly for (200) plane, Eq (2.4) can be written as:

$$a = \frac{\lambda}{sin\theta} \tag{2.5}$$

Equation (2.5) can be used to estimate the lattice constant ***c***.

The ZnO bond length can be calculated from Eq (2.6).

$$L = \sqrt{\left(\frac{a^2}{3} + \left(\frac{1}{2} - u^2\right)c^2\right)} \tag{2.6}$$

Where u called the positional parameter in wurtzite structure, measures the amount of displacement of each atom along c-axis and given by:

$$u = \frac{a^2}{3c^2} + \frac{1}{4} \tag{2.7}$$

The dislocation density of ZnO NPs will be calculated from the Eq (2.8).

$$\delta = \frac{1}{D^2} \tag{2.8}$$

Where δ is the dislocation density and D is the crystalline grain size given by Sherer's formula:

$$Dp = \frac{0.9\lambda}{\beta Cos\theta} \tag{2.9}$$

Where D is crystalline size, λ is wavelength, β is full-width at half-maximum (FWHM) of main intensity peak, θ is diffraction angle in radians.

Electronic band-gap properties of ZnO NPs

A typical semiconductor has populated states called valence bands and unpopulated states termed as conduction bands. The energy difference between valence band and conduction bands are defined as band gap which is an important property of a semiconductor; lowest energy point in the valence band is called band edge. As shown in Figure 3, there are two types of band gaps namely, direct band gap and indirect band gap; in the case of direct band gap, the minimum energy point in the conduction band has the same k value (crystal momentum) as that of the maximum energy point in the valence band while this is not case for indirect band gap semiconductor as explained in Figure 3.

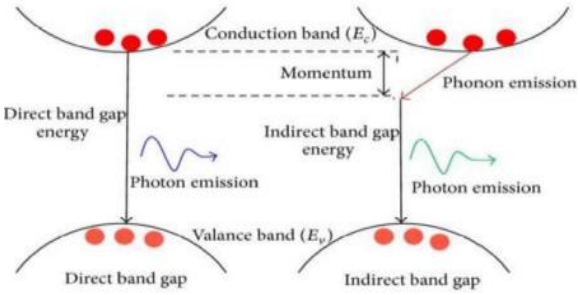

Figure 3: Direct and indirect band gap in semiconductor (Sharma & Singh, 2009)

Excitation/de-excitation in the direct band gaps are a single step process while it is a two-step process involving phonons in the case of indirect band gap semiconductors. Spectroscopic techniques are used to determine the band gap experimentally; it is straight forward for a direct band gap semiconductor while in indirect band gap semiconductor, one has to perform additional

experiments like temperature variation to estimate the band gap. Rare earth elements are widely exploited for doping nanomaterial's and to properly modify the electronic band structure. As highlighted in the work of Cerrato et al. Upon UV light irradiation, ZnO presents the very fast recombination of a photo generated charge carriers. This results in low quantum efficiency when this system is used as a photo catalytic. ZnO NPs has wide band gap of 3.37eV (direct band gap).

Optical properties of ZnO

The mechanism responsible for optical properties of a typical semiconductor is attributed to both intrinsic and extrinsic effects. Transitions associated with the emission of photons do occur between the electrons in the conduction band and holes in the valence band. These transitions include the exciton effects arising due to the Coulomb interaction; the group velocity of the electron should be equal to that of the hole. Any particular, exciton could be free or bound depending on the nature of interaction responsible for its formation.

The processes of optical absorption and emission have been influenced by an extrinsic transition called bound exciton. This bound exciton is related to defects which are responsible for creating discrete electronic states in the band gap. Exciton can be bound with neutral or charged donors and acceptors and it depends on the band Structure of semiconductor material. Zinc oxide films which made from single crystal can be applied for modulation of UV radiation due to its directionally dependent optical property. Fluorescence spectra of ZnO nanowire shows increase of green emission intensity with a decrease of nanowire diameter and continuous reduction of diameter of ZnO nanowire gives quantum size effect and due to this size confinement exciton binding energy is enhanced. The performance of optoelectronic devices have been influenced by transport characteristics and interaction of phonon with free carrier.

Physical properties of ZnO

Nanotechnology applications are greatly depending on the fundamental properties of the nanomaterial. Therefore, knowing the fundamental physical properties of ZnO is crucial to the rational design of functional devices. It should be noted that as the dimension of

the semiconductor materials shrink down to nanometer scale, some of their physical properties undergo changes due to "quantum size effects".

Table 1: Main properties of the Wurtzite ZnO structure (Hussain, 2008).

Properties		Values
Lattice parameter	*a*	3.2495 Å
	c	5.2096 Å
	c/a	1.602 (ideal hexagonal structure 1.633)
	U	0.345
Density		5.606 gcm^{-1}
Energy band gap (300K)		3.37eV (direct band gap)
Exciton binding energy		60.00meV
Magnetic susceptibility (χ)		-27.2 x 10^{-6} cm^3mole^{-1}
Electron mobility		200 $cm^2V^{-1}s^{-1}$
Hole effective mass		0.59
Electron effective mass		0.24
Hole mobility (T=300K)		5.50cm^2 $V^{-1}s^{-1}$

2.2 Synthesis Methods of ZnO Oxide NPs

There are different methods of synthesizing ZnO oxides NPs. The following are some of the methods to synthesizing NPs.

Chemical Vapor Deposition (CVD)

Chemical vapor deposition (CVD) is a widely used materials processing technology in which thin films are formed on a heated substrate via a chemical reaction of gas-phase precursors. CVD offers a clear advantage by relying on chemical reactions that enable tunable deposition rates as well as high quality products with excellent conformity. Irrespective of the variations in CVD types, the fundamental process is similar and consists of the following common elementary

steps. First, the reactant gases are transported into the reactor. These reactant gases then either undergo gas-phase reactions to form intermediate reactants and gaseous by-products via homogeneous reactions or diffuse directly through the boundary layer to the substrate. In both cases, the reactant gases and the intermediate reactants adsorb onto the heated substrate surface and diffuse on the surface.

The subsequent heterogeneous reactions at the gas–solid interface lead to continuous thin film formation via nucleation, growth and coalescence as well as formation of reaction by-products. Finally, any gaseous products and unreacted species desorb from the surface and are carried away from the reaction zone. The gas-phase reactions occur when the temperature is sufficiently high or additional energy is introduced, for example, in the form of plasma (Sun & Hong, 2021).

Co-Precipitation Method

Co-precipitation method refers to obtain uniform composition in two or more captions homogeneous solution through precipitation reaction, is one of important methods for the synthesis of composites containing two or more kinds of metal elements. There are four types of co-precipitation: surface adsorption, mixed crystal formation, occlusion and mechanical entrapment. ***Surface adsorption*** takes place for precipitates with larger surface areas. Specially coagulated colloids contaminate by this method. In ***mixed- crystal formation***, one of the ions in the crystal lattice is replaced by another ion. Surface adsorption and mixed- crystal formation are equilibrium processes, whereas the other two are kinetic phenomena. When a crystal is growing rapidly, contaminant can trap inside the growing crystal and this is known as ***occlusion***. ***Mechanical entrapment*** is the mechanism where some amount of solution is trapped inside the crystals. This happens when two growing crystals are close together, so that they grow together (Choy, 2003).

Precipitation Method

Precipitation is the process of transforming a dissolved substance into an insoluble solid from a super-saturated solution. Sometimes solids are a result of a chemical reaction in a solution. These solid particles will eventually settle down due to their density, and it is known as a precipitate. In centrifugation, the resulting precipitated is also known as the pellet. The solution

above the precipitate is known as the supernatant. In the precipitate, the particle size changes from time to time (Yan et al., 2013).

Colloidal suspensions contain tiny particles, which do not settle down, and cannot be easily filtered. Crystals can be easily filtered, and they are larger in size. However, it has been found that the particle size of the precipitate is influenced by precipitates' solubility, temperature, reactant concentrations and rate at which reactants are mixed.

Seeding method

The seeding method was discovered by Frens (1972, 1973), where nanoparticles are grown by the reduction of salt in aqueous solution which contains seed nanoparticles. In this method, the stabilizers are used to control the size and shape of growing nanoparticles. This method was developed over the years using various types of seeding, reducing agents, and stabilizer. For example, the method which was developed by Perrault and Chan in 2009 reduces HAuCl in gold nanoparticles seed-contained aqueous solution using hydroquinone. The gold nanoparticle seed can act in conjunction with hydroquinone to catalyze the reduction of gold ions into their surface. If the stabilizer is citrate, typically the seed nanoparticles were prepared by the citrate method. Using this method, the size of nanoparticles can be grown at least 30–300 nm.

Sol-gel Method

Sol-gel processing is bottom up technique, which is used to the field of material science and ceramic engineering for the generation of oxide Nano powder and composite NPs from a sol followed by a gel formation. Sol-gel refers to typical chemicophysical properties owned by materials, which makes them possible to be exploited in technological applications includes electrical conductors, thermo electrics, ferroelectrics, magnet and transparent optical devices.

Sol is a system of tiny solid particles suspended in the liquid phase and constantly showing Brownian movement. Because Gibbs free energy of the interface atom is higher than that of internal atoms, the sol is thermodynamically unstable. The particle tends to agglomerate spontaneously, reaching a low surface energy state. Gel is kind of solid feature of the colloidal system composed of fine particles in three dimensional network structures and a continuous medium consisting of dispersed phase. Gelation process can be regarded as a small particle

cluster connected to each other as a continuous solid network. Sol-gel process is mainly based on hydrolysis and condensation reactions of metal alkoxides, the molecular precursors that develop an oxide network in a liquid medium. Sol-gel process functionally opens promising applications in many areas: solar cells, biology, and medicine (e.g. as membrane and separation devices), fuel, energy, ionic, catalysis, sensors, functional smart coating. Sol-gel derived coatings provide a wide range of applications: corrosion protective, hydrophilic and hydrophobic, anti-reflective and anti-fog coatings, migration barriers against liquid and volatile compounds, anti-bacterial modification of textiles and water repellent antistatic textiles and self-cleaning coatings.

Hydrothermal Method

In the hydrothermal method, the crystals of nanoparticles are grown by heterogeneous reaction under conditions of high temperature and high pressure from substances which are insoluble at normal temperature and pressure. The crystal growth is carried out in an apparatus consisting of a steel pressure vessel called an autoclave, in which nutrients are supplied along with water. Hydrothermal synthesis is usually carried out below 300°C. The critical condition gives a favorable reaction field for formation of nanoparticles, owing to the enhancement of the reaction rate and large super saturation based on the nucleation theory. This method has been used to synthesize metal oxide nanoparticles in supercritical water, metal nanoparticles, and semiconductor nanoparticles (Herizchi et al., 2016).

Green Synthesis of Zinc Oxide Nanoparticles

Green synthesis procedures involve the plant based synthesis of nanoparticles. Green synthesis techniques make use of somewhat pollutant free chemicals for synthesis of nanostructures. It embraces the use of ecofriendly and safe solvents such as water, natural extracts. Biological approaches using microorganisms and plants or plant extracts for synthesis of metal nanoparticles have been suggested as safe alternatives of chemical methods. In biogenic synthesis of nanoparticle, several biological systems including bacteria, fungi, and yeast has been used safely. But synthesis of nanoparticles by using microorganisms is difficult because it involves elaborate process of maintaining cell cultures, intracellular synthesis, and multiple purification steps.

Synthesizing ZnONPs Using Leaf Extract of *Melia azadarach*

Melia azadarach commonly known as Cape Lilac and locally as Moringa or Shiferra belongs to the family *Meliaceae* . It is native to Southeast Asia and found naturally in most of the tropical and subtropical countries. This plant is locally famous for its anti-microbial, anti-inflammatory and anti-cancer activities and often used to treat stomach pains and parasitic infections. It produces dense array of dark green leaves which are short stalked and arranged in alternate pattern on terminal branches. Fruits are yellow colored, smooth and fleshy berries. *M.azadarach* is naturally enriched in phytochemicals. It is endowed with alkaloids, sterols, glycosides, flavonoids, limonoids, fixed oil and fats, phenolic compounds, tannins, saponins, gum and mucilages, triterpenes, azadirachitin, nimbin, melianoninol, melianol, meliandiol, vanillin, meliacin, quercertin and rutin (Naseer et al., 2020). Due to the presence of diverse array of these phytochemicals and medicinal properties, *M. azedarach* hold greater potential for efficient biosynthesis of NPs that can be useful to treat clinical pathogens.

For synthesis of ZnO NPs, 95 mL of 0.01 M zinc acetate dehydrate (Zn $(C_2H_3O_2)_2.2H_2O$) solution was mixed with 5mL plant extract *M. azadarach* in 250 mL flasks. These mixtures were incubated at 70°C for 1hour with continuous shaking at 150 rpm. This led to the settlement of bio-reduced salt at the bottom of the flask which appeared as white precipitate. The supernatant was decanted and powdery precipitate was transferred to 1.5 mL centrifuge tubes. The samples were subjected to washing with d.H_2O by centrifugation at 3000 rpm (revolution per minutes) for 30 minutes. Washing step was repeated thrice to ensure removal of impurities (Han, 2011).

Synthesizing ZnO NPs Using Aqueous Leaf Extracts of Coffee (*Coffee Arabica*)

The coffee plant is a climber of one to seven meters long, and it has opposite sided leaves with bulbous moods on both edges. The parts that are commercially used are the leaves, seeds, and stems. The leaf of coffee is not functional and no studies were conducted in our country Ethiopia, and they simply drop to the ground and lead to environmental toxicity (Rajiv et al., 2013). Using this leaf regard less of its seed incorporation reduces toxicity of the water, air, and environment (Abel et al., 2021).

The main constituents of coffee are caffeine, tannin, fixed oil, carbohydrates, and proteins. It contains 2–3% caffeine, 3–5% tannins, 13% proteins, and 10–15% fixed oils. In the seeds, caffeine is present as a salt of chlorogenic acid (CGA) and contains oil and wax. Coffee is often

used as antioxidants, but more importantly coffee is a good source of chromium and magnesium that assist in controlling blood sugar by ensuring proper usage of insulin.

Preparation of ZnO NPs

The precursor basis for the zinc ion used in this study was zinc-nitrite hydroxide which was taken from shops from Finfinnee, Ethiopia. The elucidation of zinc-nitrite hydroxide was set in deionized water. For synthesize of ZnO nanoparticles, the flask volume of 250 mL and the source of zinc (0.1 M) was mixed with 20 mL of the leaf extract of the coffee leaf and stimulated on a magnetic stirrer heated at 80°C , and the stirring was nonstop until a uniform solution was accomplished . The homogenous solution was dehydrated in a hot air oven at the temperature of 120-150°C for 120 min. The color of prepared nanoparticles is yellow and is crumpled in a metallic mortar-pestle to get a green preparation of ZnO nanoparticles.

Synthesizing ZnO NPs Using Orange fruit peel Extract

Orange fruit is one of the most productive fruit in the world. Orange fruit peel, as the main by-product of citrus, is rich in a variety of natural anti-oxidants. Therefore, the extract of orange peel is considered to be used as a stabilizer to prepare ZnO NPs (Doan Thi et al., 2020)

Preparation of ZnO NPs

The ZnO NPs were synthesized by mixing 2g of zinc nitrate with 42.5 mL of each of the extracts. These mixtures were then stirred for 60 minutes and then placed in a water bath at 60^{o}C for 60 minutes. Subsequently, the mixtures were dried at 150 ^{o}C and then heat-treated at 400 ^{o}C for 1 hour. The organic substances (Flavonoid, Limonoid, Carotenoids) in orange peel extract act as ligand agents. The mixture of organic solution is then decomposed directly when calcination at 400 ^{o}C resulting in the release of ZnO nanoparticles.

All of the above plant extract for the synthesis of ZnO NPs were tested on different types of bacteria. Among them, ZnO NPs synthesized by using leaf extract of *M.azadrach* shows a better advantage against the two bacteria, E.coli (Gram Negative) and S.aureus (Gram Positive).

2.3 Green Synthesis of Silver (Ag) NPs Using *Allium Sativum* (Garlic) Extract

A common approach for green nanoparticle synthesis at ambient temperature is to begin with naturally available resources containing phytochemicals that function as both the reducing and stabilizing agents (Philip, 2009). Philip et al. synthesized around 15 nm diameters of gold nanoparticles in aqueous media by using honey (Shukla et al., 2008). Shukla et al. used soy bean extracts to produce nontoxic gold nanoparticles and suggested that they are ideal for use in Nano medicine as a result of their stability in various biological media and invitro compatibility (Gardea-torresdey et al., 2003). Other studies of silver and gold nanoparticle synthesis have employed herbal extracts from alfalfa, lemongrass, and green tea, where the natural extracts serve as both reducing and stabilizing agents (Von White et al., 2012).

Gregory Von White II et al. synthesized silver NPs (4-6 nm) by using garlic (*Allium Sativum*) extract as the reducing and stabilizing agents. According to Gregory Von White II et al, it is possible to control the size and size distribution of silver NPs by varying the synthesis condition of garlic extract concentration and temperature (Smuleac et al., 2011).

CHAPTER 3 MATERIALS AND METHODS

3.1 Materials and Chemicals

Materials

The materials used for the synthesis were, fresh root of *Zingiber officinale* and Garlic Bulb (*Allium Sativum*) purchased from local market, Beaker, Magnetic Stirrer, Hot plate, Incubator, Power supply, Thermometer, Whattman No.1 filter papers, Digital electrical analytical balance (Model FA2104, China) Furnace (Model BK-5-12GJ), Ceramic crucible cups, Drying Oven (Model 101-0, Biobase Biodustry, Shadong, Co.Ltd), Cylinders, Centrifuge (Model AVI-558, Max RPM:5000 rpm).

Chemicals

The chemicals used for the synthesis were includes: Zinc acetate (Zn $(CH_3COO)_2 .2H_2O$, Molar: 219.49 g/mol, Merk Life Science PLC), Deionized water (Dallul Pharmaceuticals PLC, Finfinnee, Ethiopia), Distilled water (Adama Science and Technology university, Adama, Ethiopia), Ethanol and Sodium hydroxide (NaOH) (Cas no. 1310-72-2, Minimum assay 99.0%, Neolab Life Science Co.Ltd). Zinc acetate dehydrate was provided as precursors and sodium hydroxide was used for controlling the pH values. All the reagents using in the experiments will be in analytical grade and used without any further purification.

3.2 Experimental Methods

Preparation of the Extract

Fresh root of *Z.officinale* and garlic were purchased from local market. *Z.officinale* was washed thoroughly within distilled water and soaked in distilled water for 20 minutes in order to remove the contaminant present in the skin. In the same manner, garlic was washed thoroughly within distilled water after the outer skin pilled off. The roots were completely air dried and the moisture contents were removed. The dried roots were crushed by using mortar and pestle. Then, 10g of the powder of each sample were taken and boiled for 30 min. Finally, the extracts were filtered by Whatman No.1 filter paper and stored at 4^oC for further use.

Synthesis of ZnO NPs

4g of Zinc acetate (Zn $(CH_3COO)_2$. $2H_2O$) was added into 50mL of deionized water (DW) to get final concentration of Zinc acetate dehydrate (Zn $(C_2H_3O_2)_2.2H_2O$). 10mL of *Z.officinale* root extract and garlic extract were slowly added to Zinc acetate dehydrate solution in the different beaker and 10mL their mixtures were added to Zinc acetate dehydrate solution in the same ratio. The mixtures were heated and stirred on magnetic stirrer for 2hr at 50 ^oC until the white precipitate were observed. Then, the pellets were centrifuged three times for 10 min interval at 5000 rpm and dried in an Oven for overnight at 80 ^oC. Then, the dried samples were calcined in a Muffle furnace at 450 ^oC for 2hr and the powders were collected for characterization.

3.3 Characterization Techniques

The laboratory instruments used for characterization of ZnO NPs are X-ray Diffraction (XRD) (X-ray target tube, Cu-kα radiation, 40 kV, Scanning rate 3^o min^{-1}, recorded 2θ range between 10^o- 80^o) used to study the crystal structure. UV-Visible Spectroscopy (UV-3600Plus Series, Measuring absorbance mode, Slit width 2nm) employed to investigate the optical properties of the sample and the peak emission of nanoparticles studied by Photoluminescence (PL) Spectroscopy (Cary Eclipse Fluorescence Spectrophotometer, scan rate 600 nm/min, MY18490002, Agilent Technologies, Malaysia). The surface chemistry (functional groups) of synthesized ZnO NPs was characterized through FTIR spectroscopy (IS50, APX, Germany).

3.4 Antibacterial Activities

The antibacterial activities of ZnO NPs was tested against standard pathogens of Gram negative (E.coli-ATCC 9637 and P.putida-ATCC 47054) and Gram-Positive (S.aureus-ATCC 6538 and S.pyogenes-ATCC 19615). Antimicrobial activities were carried out through Disc diffusion method on Muller Hinton Agar (MHA at concentration about $5x10^5$ CFU/mL) medium containing petri plates. Ampicillin was used as positive control in each plate. The plates were incubated for 18 hr at 37^oC. Stock solution of synthesized ZnO NPs was prepared in Dimethyl Sulfoxide (DMSO, C2H6OS, 99.9 % Pure, Loba Chemie PVT.LTD) at different concentrations of 15 mg/mL, 10 mg/mL, and 5 mg/mL.

Figure 4 indicates the summary diagram of ZnO NPs synthesized using Garlic Bulb (*Allium sativum*) extract, *Z.officinale* root extract and their mixture. The diagram shows the laboratory activities of synthesized ZnO NPs.

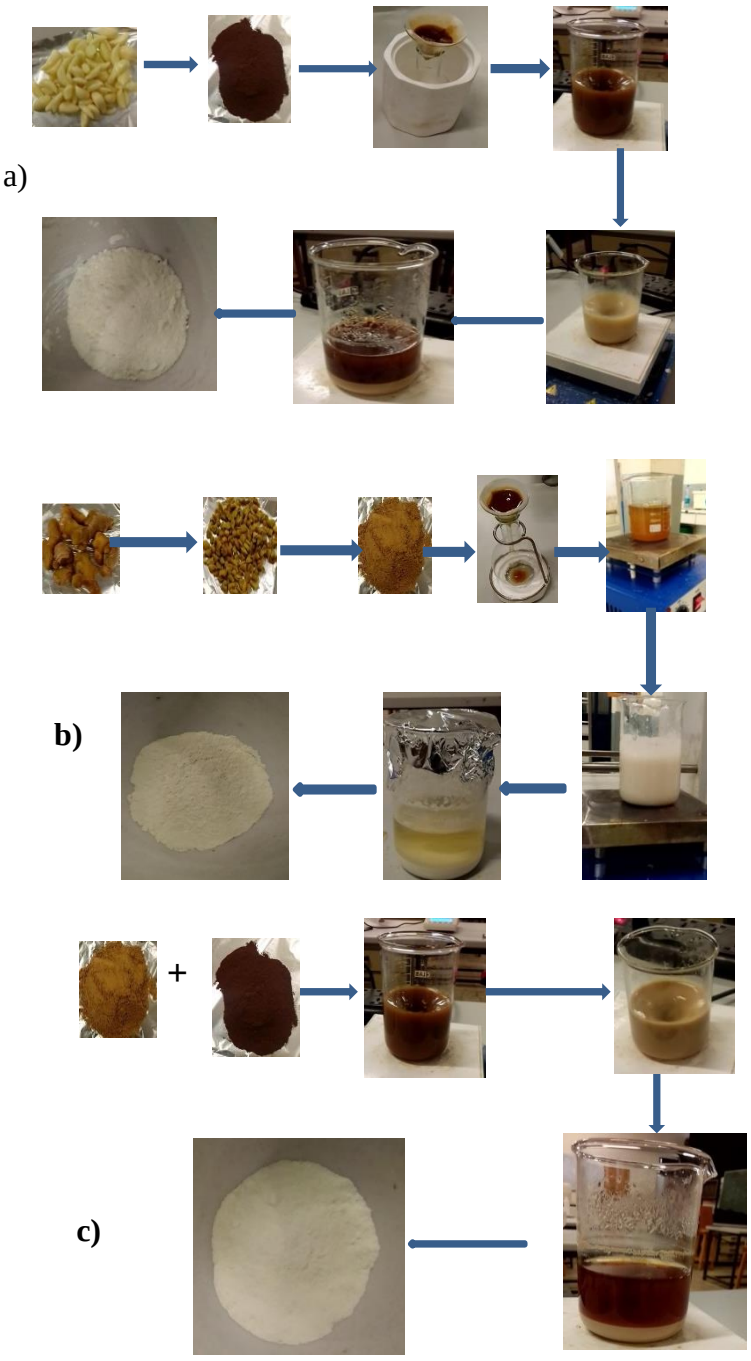

Figure 4: Summary diagrams of ZnO NPs synthesized using a) Garlic Bulb extract, b) *Z.officinale* root extract and c) *Z.officinale* root and Garlic Bulb extract (their mixture).

CHAPTER 4 RESULTS AND DISCUSSIONS

4.1 XRD Analysis

X-ray diffraction patterns of synthesized ZnO NPs peaks were agreed with the data (JCPDS card No. 00-036-1451). Figure 5 shows the characteristic Bragg diffraction at 2θ values of three samples. The first one is ZnO NPs synthesized using Garlic Bulb extract indicates the distinctive Bragg diffraction at 2θ values of 31.7655, 34.4285, 36.2442, 47.5393, 56.0257, 56.5899, 62.8650, 66.3949, 67.9559, 69.0486 and 77.0918 with strongest peaks 2θ= 36.2442, 31.7655 and34.4285. The second sample is ZnO NPs synthesized using *Z.officinale* root extract shows the distinctive Bragg diffraction at 2θ values of 31.2218, 31.7853, 34.0788, 34.4416, 36.2623, 36.9362, 44.0242, 47.5563, 56.6106, 62.2836, 62.8783, 64.3850, 66.3939, 67.9660, 69.0980, 76.9593 and 77.4670 with the strongest peaks 2θ = 36.2623, 31.7853 and 34.4416. The third one is ZnO NPs synthesized using *Z.officinale* root extract and Garlic Bulb extract shows the distinctive Bragg diffraction at 2θ values of 31.7932, 33.9189, 34.4504, 36.2741, 36.8563, 47.5664, 56.0657, 56.6233, 57.1853, 62.4235, 62.8890, 66.4105, 67.9762 and 69.0932 with the strongest peaks 2θ = 36.2741, 31.7932, and 34.4504. They were indexed to the plane (100), (002), (101), (102), (110), (103), (112), (200), and (201) that are in good agreement with wurtzite ZnO structure. The distinct and clear peaks confirmed the high purity and crystalline nature of the prepared ZnO NPs. The crystalline size has been estimated from the broad diffraction peak using the Debye–Scherer formula (Shanmugapriya et al., 2019):

$$Dp = \frac{0.9\lambda}{\beta Cos\theta} \tag{4.1}$$

Where D is the crystal size of ZnO NPs, k is Scherer's constant given by 0.9, λ is the wavelength of X-rays (1.541 Å), θ is the Bragg diffraction angle, and β is the full-width at half-maximum (FWHM) of the diffraction peak corresponding to plane (101). The average particle size of ZnO NPs synthesized using Garlic Bulb (*Allium Sativum*) extract, *Z.officinale* (Ginger) root extract and their mixture were found to be 19.8nm, 21.94nm, 23.86 nm, which were derived from the FWHM of the more intense peak (β = 0.42200, 0.38080, 0.35010) corresponding to the (101) plane located at 2θ = 36.2442^o, 36.2623^o, 36.2741^o respectively.

The average particle size of synthesized ZnO NPs obtained from XRD data shows good results compared to the previous report. Raja, L.F.A studied the effect of ZnO NPs produced by *Z.officinale* against pathogenic bacteria and was reported the average particle size as 30 nm (Anand Raj & Jayalakshmy, 2015). Vidya, C. et.al was synthesized ZnO NPs by using *Calotropis Gigantea* and has reported the average grain size as 30-35 nm. Yuvakumar,R. et.al was synthesized ZnO NPs using noble plant rambutan (*Nephelium lappaceum L*) peel extract and has been reported the average crystalline size as 50.95 nm (Yuvakkumar et al., 2014).

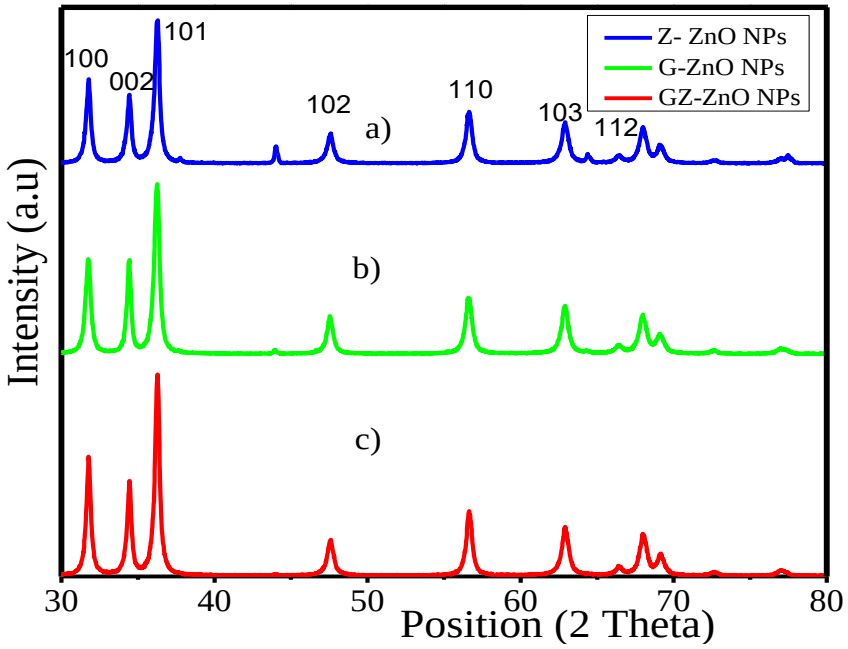

Figure 5: XRD patterns of ZnO NPs synthesized using: A) *Z.officinale* (Z) root extract, B) Garlic Bulb (G) extract, C) the mixture of *Zingiber Officinale* root and Garlic Bulb (GZ) extract.

4.2 Photo luminescent (PL) Spectrum

Figure 6 indicates the PL spectrum (peak emission) of ZnO NPs synthesized using *Z.officinale* root extract, Garlic Bulb extract and their mixture. A broad blue emission peak centered at (421.05 nm), (393 and 420 nm) and (421.95 nm) can be observed for ZnO NPs synthesized using *Z.officinale* root extract, Garlic Bulb extract and their mixtures respectively. From the evidence of given data (figure 6) the different peaks exists at different wavelength, which were normally associated with Zn defects, such as transitions of an electron from *conduction band to the valance band and* O_2 vacancies. The O_2 vacancies change the properties of oxide materials by producing F centers ionic oxides which may cause the formation of metal-metal bonds in

covalent bond. In other case, O_2 vacancies changing the oxidation state of compounds of transition metal atoms with empty d orbitals, which can eventually altering the local electronic structure of atoms (Manju et al., 2020).

In n-type ZnO, acceptor-like defects (O_2) are easier to form, which enables the transition between different band-gap energies (Alamdari et al., 2020). The PL emission rate is directly proportional to the photo-excited load carrier's recombination probability. Higher PL Strength advanced e−/h+ pair (electron hole pair) recombination and guides to the lower photocatalytic activity (Khan et al., 2021).

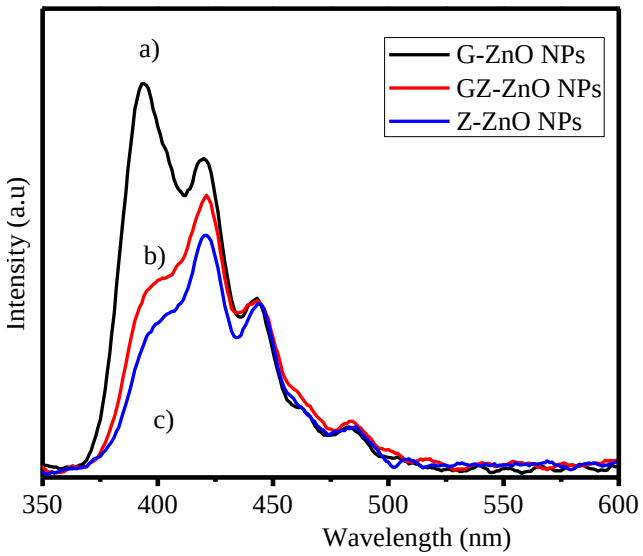

Figure 6: PL Spectrum (peak emission) of ZnO NPs synthesized ZnO NPs synthesized using: a) Garlic Bulb (G) extract, b) the mixture of Garlic Bulb and *Z.officinale* root extract (GZ), c) *Z.officinale* (Z) root extract at excitation wavelength of 325 nm respectively.

4.3 UV-Vis Absorbance

Figure 7 shows the UV-vis absorbance of ZnO NPs synthesized by using *Z.officinale* root extract, garlic extract and their mixture. The optical band gap energy of ZnO NPs synthesized by using *Z.officinale* root extract, Garlic Bulb extract and their mixture calculated by using the relation (E_g = hv) were found to be 3.3eV, 3.375eV, 3.325eV at maximum wavelength of 377.5nm, 369.5nm and 374nm respectively.

The calculated band gap energy of synthesized ZnO NPs were performs good agreement with the optical band gap energy of standard ZnO NPs that was found to be 3.37 eV.

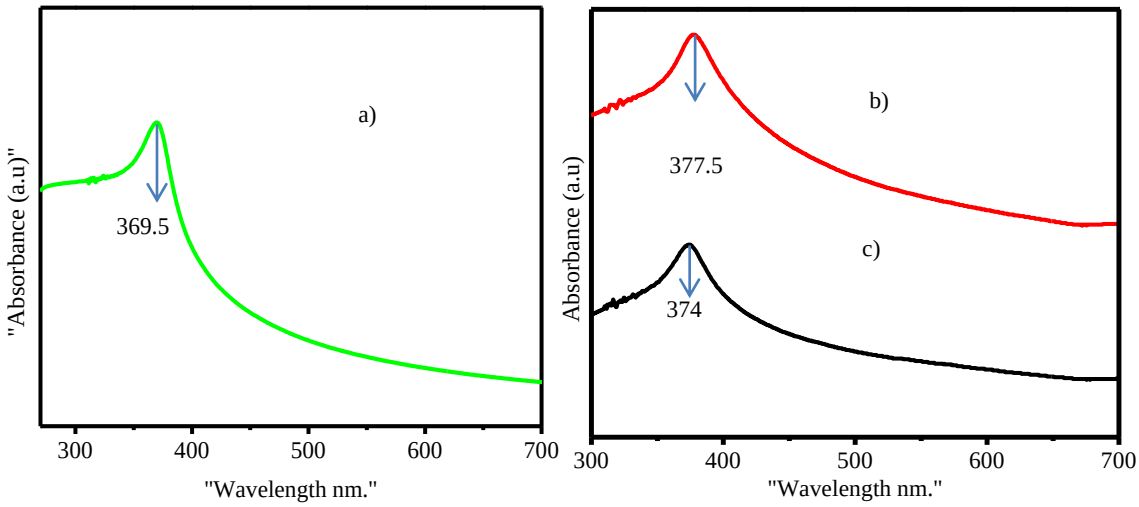

Figure 7: UV-Vis absorbance spectrum of ZnO NPs synthesized by using; a) Garlic Bulb extract, b) *Z.officinale* root extract, c) the mixture of Garlic Bulb and *Z.officinale* root extract.

4.4 FTIR Analysis

FTIR spectrometry was performed to identify the functional groups associated with the ZnO NPs formation. Figure 8 (a, b, c) represent the FTIR spectrum of ZnO NPs synthesized using Garlic Bulb extract, *Z.officinale* root extract and their mixture respectively. ZnO NPs absorption band was obtained within the region 4000-400 cm^{-1}. The bands at 913.09 cm^{-1}, 919.16 cm^{-1} and 915.55 cm^{-1} in FTIR spectrum confirms the formation of ZnO NPs synthesized using Garlic Bulb extract, *Z.officinale* root extract and their mixtures respectively (Kulkarni, 2015). Broad band at 3400- 3200 cm^{-1} showed characteristic OH. The bands at may be proposed the N-H stretching of amines. Bands at 1331.37 cm^{-1}, 1391.83 cm^{-1} and 1394.66 cm^{-1} confirmed the presence of carboxylic acid and aromatic C-H bending (Ikram et al., 2020). Therefore, the present studies were confirmed with the previous report.

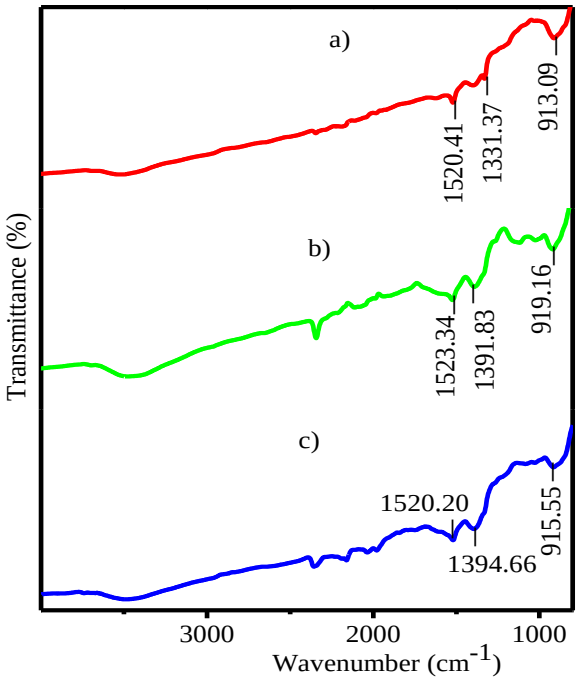

Figure 8: FTIR spectrums of ZnO NPs synthesized using a) Garlic Bulb extract, b) *Z.officinale* root extract and c) the mixture of Garlic Bulb and *Z.officinale* root extract respectively.

4.5 Antibacterial Activities

The bactericidal activities of ZnO NPs synthesiszed using Garlic Bulb extract, *Z.officinale* root extract, and their mixtures were tested against two main standard phathogenes known as Gram negative (G-ve) and Gram positive (G+ve) bacteria. From Gram Negative bacteria, Escherichia coli (E.coli) and Pseudomonas putida (P.putida) and from Gram Positive bacteria, Staphylococus aureus (S.aureus) and Streptococus pyogenes (S.pyogenes) were grown to test the antimicrobial activities of synthesized ZnO NPs.

According to the evidence of zone of inhition of the recorded data (Figure 10, Table 2), ZnO NPs synthesized by using the mixtures of garlic and *Z.officinale* root extract (GZ) was more effective on the G-ve bacteria P.putida (28.67$\pm$0.82 mm) and E.coli (15.3$\pm$0.94 mm) copared to G+ve bacteria S.pyogenes(10.67 $\pm$0.47 mm) and S.aereus (15.67$\pm$ 0.82 mm). Garlic mediated ZnO NPs was more significant on G-ve bacteria P.putida (21.67$\pm$0.88 mm) and E.coli (19$\pm$0.82 mm) compared to G+ve bacteria S.aureus (17.7 $\pm$0.47 mm) and S.pyogenes (7$\pm$0.82 mm). (Figure 9, Table 3). ZnO NPs synthesized by using *Z.officinale* root extract was more effective

on G+ve bacteria S.aureus (16.4±0.47 mm) and S.pyogenes (10±0.82 mm) compared to G-ve bacteria P.putida (7.7 ±0.78 mm) and E.coli (4±1.00 mm). (Figure 11, Table 4). However, it is possible to say that the zone of inhibition of the mixture of garlic and *Z.officinale* (GZ) mediated ZnO NPs was greater than that of Garlic Bulb (G) mediated ZnO NPs and *Z.officinale* root extract (Z) mediated ZnO NPs against G-ve bacteria like P.putida. These results suggest that the use of ZnO NPs synthesized by using the mixture of garlic and *Z.offinale* root extract can be more efficient against Gram negative bacteria (G-ve). This might be due to the presence of higher number of phenolic compounds and rare secondary metabolites present in both Garlic Bulb and *Z.officinale* root. Renata, D. and J. Dhugaszewska reported that ROS (reactive oxygen species) such as superoxide and hydroxyl radicals produced by ZnO NPs were cause damage of bacterial cell membrane (Dobrucka & Długaszewska, 2016).

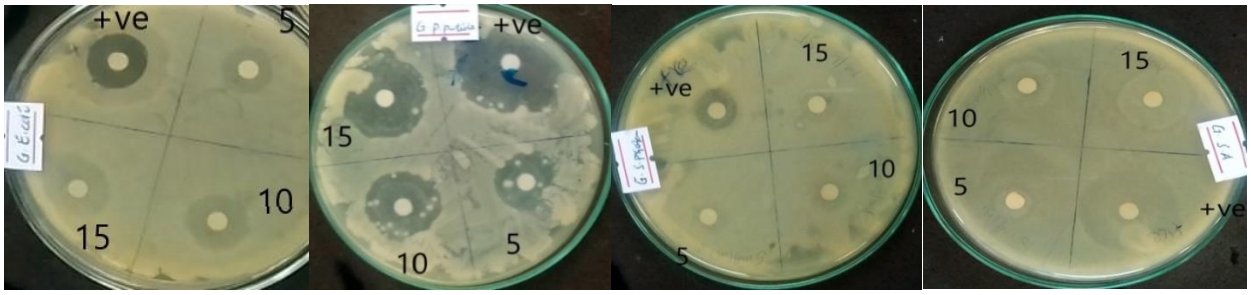

Figure 9: Antimicrobial activities of ZnO NPs synthesized by using Garlic Bulb extract against E.coli, P.putida, S.pyogenes, S.aureus respectively.

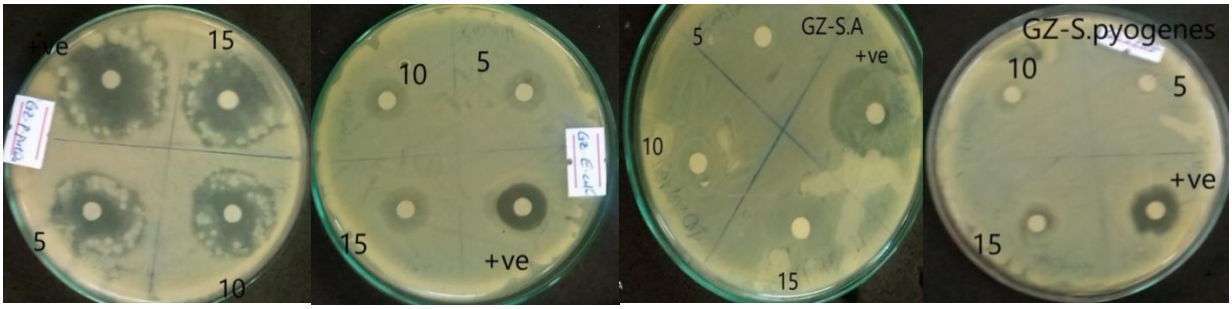

Figure 10: Antimicrobial activities of ZnO NPs synthesized by using the mixture of Garlic Bulb extract and *Z.officinale* root extract against P.putida, E.coli, S.aureus And S.pyogenes respectively.

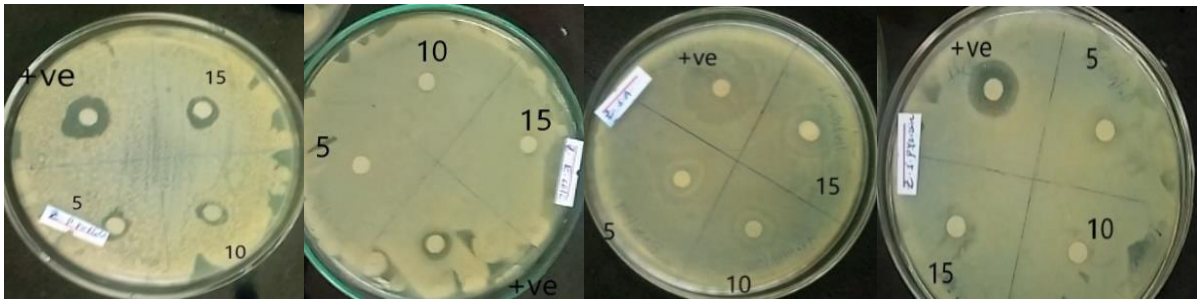

Figure 11: Antimicrobial activities of ZnO NPs synthesized using *Z.officinale* root extract against P.putida, E.coli, S.aureus and S.pyogenes respectively.

Figure (9, 10 and 11) shows antimicrobial activities of Synthesized ZnO NPs against G-ve bacteria (P.putida and E.coli) and G+ve bacteria (S.aureus and S.pyogenes) at different concentrations of 5 mg/mL, 10 mg/mL, 15 mg/mL. As the concentration of sythesized NPs increased, the zone of inhibition also increased.

Table 2: Antibacterial activities of ZnO NPs synthesized using mixture of Garlic Bulb and *Z.officinale* root extract (GZ) at different concentration.

Bacterial Species	**Zone of inhibition (mm)**			
	G Z – ZnO NPs			**Positive Control**
	5mg/mL	**10 mg/mL**	**15mg/mL**	
P.putida	24±0.82	24.7±0.94	28.67±0.82	29±1.63
S.aureus	9±0.82	11±0.82	15.67±0.82	21.3±1.24
P.pyogenes	7.4±0.94	9±0.82	10.67±0.47	14.7±0.47
E.coli	12.3±1.7	13±0.82	15.3±0.94	17±1.63

Table 3: Antibacterial activities of ZnO NPs synthesized by using Garlic Bulb (G) extract at different concentration.

Bacterial Species	**Zone of inhibition (mm)**			
	G – ZnO NPs			**Positive Control**
	5mg/mL	**10 mg/mL**	**15mg/mL**	
P.putida	18.67±0.88	21±1.41	21.67±0.88	24.7±0.94
S.aureus	11.7±1.24	13.4±0.47	17.7±0.47	24±0.82
P.pyogenes	5±0.82	6.7±0.47	7±0.82	11.4±0.58
E.coli	11.67±1.24	13.67±0.47	19±0.82	19.3±1.89

Table 4: Antibacterial activities of ZnO NPs synthesized by using *Z.officinale* root (Z) extract at different concentration.

Bacterial Species	**Zone of inhibition (mm)**			
	Z – ZnO NPs			**Positive Control**
	5mg/mL	**10 mg/mL**	**15mg/mL**	
P.putida	6±0.82	6.4±0.48	7.7±0.78	9±0.00
S.aureus	10±0.82	14.4±0.47	16.4±0.47	19±1.63
P.pyogenes	5±2.16	6±0.57	10±0.82	14.7±0.94
E.coli	2±0.00	2.7±0.78	4±1.00	9±0.00

CONCLUSION AND RECOMMENDATION

Conclusion

Green synthesis of ZnO NPs has more advantages than other methods. This is because of cost effective, ecofriendly, and non-toxicity of plant extract. ZnO NPs using *Z.officinale* root extrct, Garlic Bulb extract and their mixture were successfully synthesized. According to the evidence presented in the Table (2) we can observed that ZnO NPs synthesized by using the mixture of Garlic Bulb and *Z.officinale* root extract shown high inhibition zone against P.putida (28.67±. 0.82). This might be due to the presence of higher number of phenolic compounds and rare secondary metabolites present in both Garlic Bulb and *Z.officinale* root. The XRD examinations of synthesized ZnO NPs were confirmed the formation of wurtzite shape NPs. The absorption spectrum of ZnO NPs synthesized using Garlic Bulb extract; *Z.officinale* root extract and their mixture were found to be 369.5 nm, 377.5 nm and 374 nm with the band gap of 3.7 eV, 3.3 eV, and 3.325 eV respectively. The bands at 913.09 cm^{-1}, 919.16 cm^{-1} and 915.55 cm^{-1} in FTIR spectrum confirms the formation of ZnO NPs and the PL spectrum centered at 421.06 nm, 421.96 nm, 421.95 nm shows the peak emission of ZnO NPs synthesized using Garlic Bulb extract; *Z.officinale* root extract and their mixture respectively.

Recommendation

We have synthesized ZnO NPs using green synthesis method. Green synthesis using plant extracts are cost effective, ecofriendly and save nature of the resulting NPs. Because of these, green synthesis of ZnO NPs is recommended for antimicrobial activities, biosensor, photocatalysis, cancer treatment, gas sensor, etc.

REFERENCES

Abel, S., Tesfaye, J. L., Shanmugam, R., Dwarampudi, L. P., Lamessa, G., Nagaprasad, N., Benti, M., & Krishnaraj, R. (2021). Green synthesis and characterizations of zinc oxide (ZnO) nanoparticles using aqueous leaf extracts of coffee (Coffea arabica) and its application in environmental toxicity reduction. *Journal of Nanomaterials*, 6, 3413350.

Alamdari, S., Ghamsari, M. S., Lee, C., Han, W., Park, H., Tafreshi, M. J., & Afarideh, H. (2020). Applsci-10-03620.Pdf. *Applied Sciences*, *10*(3620), 1–19.

Anand Raj, L. F. A., & Jayalakshmy, E. (2015). Effect of zinc oxide nanoparticle produced by Zingiber Officinale against pathogenic bacteria. *Journal of Chemical and Pharmaceutical Sciences*, *8*(1), 124–127.

Bansal, V., Poddar, P., Ahmad, A., & Sastry, M. (2006). *Room-Temperature Biosynthesis of Ferroelectric Barium Titanate Nanoparticles*. *10*, 11958–11963.

Cerrato, E., Gionco, C., Berruti, I., Sordello, F., Calza, P., & Paganini, M. C. (2018). Rare earth ions doped ZnO : Synthesis , characterization and preliminary photoactivity assessment ZnO. *Journal of Solid State Chemistry*, *264*(April), 42–47.

Chavali, M. S., & Nikolova, M. P. (2019). Metal oxide nanoparticles and their applications in nanotechnology. *SN Applied Sciences*, *1*(6), 1–30.

Choy, K. L. (2003). Chemical vapour deposition of coatings. *Progress in Materials Science*, *48*, 57–170.

Daniel, M., & Astruc, D. (2004). Gold Nanoparticles : Assembly , Supramolecular Chemistry , Quantum-Size-Related Properties , and Applications toward Biology , Catalysis , and Nanotechnology. *Molecular Nanosciences and Catalysis Group*, 104, 293-346.

Doan Thi, T. U., Nguyen, T. T., Thi, Y. D., Ta Thi, K. H., Phan, B. T., & Pham, K. N. (2020). Green synthesis of ZnO nanoparticles using orange fruit peel extract for antibacterial activities. *RSC Advances*, *10*(40), 23899–23907.

Dobrucka, R., & Długaszewska, J. (2016). Biosynthesis and antibacterial activity of ZnO nanoparticles using Trifolium pratense flower extract. *Saudi Journal of Biological Sciences*, *23*(4), 517–523.

Dönmez, S. (2020). Green synthesis of zinc oxide nanoparticles using Zingiber officinale root extract and their applications in glucose biosensor. *El-Cezeri Journal of Science and Engineering*, *7*(3), 1191–1200.

Franke, M. E., Koplin, T. J., & Simon, U. (n.d.). *reviews Metal and Metal Oxide Nanoparticles in Chemiresistors : Does the Nanoscale Matter ? 1*, 36–50.

Gardea-torresdey, J. L., Gomez, E., Peralta-videa, J. R., Parsons, J. G., Troiani, H., & Jose-yacaman, M. (2003). *Alfalfa Sprouts : A Natural Source for the Synthesis of Silver Nanoparticles*. *4*, 1357–1361.

Han, D. (2011). *Nano-zinc oxide damages spatial cognition capability via over-enhanced long-term potentiation in hippocampus of Wistar rats*. 1453–1461.

Herizchi, R., Abbasi, E., Milani, M., & Akbarzadeh, A. (2016). Current methods for synthesis of gold nanoparticles. *Artificial Cells, Nanomedicine and Biotechnology*, *44*(2), 596–602.

Hussain, S. (2008). Investigation of Structural and Optical Properties of Nanocrystalline ZnO. *The Department of Physics, Chemistry and Biology*, 93.

Ikram, M. A. M., Ul, M. I. A., & Avais, H. M. (2020). Green synthesis and evaluation of n - type ZnO nanoparticles doped with plant extract for use as alternative antibacterials. *Applied Nanoscience*, *10*(10), 3787–3803.

Kato, H. (2011). Tracking nanoparticles inside cells. *Nature Publishing Group*, *6*(3), 139–140.

Khan, M., Ware, P., & Shimpi, N. (2021). Synthesis of ZnO nanoparticles using peels of Passiflora foetida and study of its activity as an efficient catalyst for the degradation of hazardous organic dye. *SN Applied Sciences*, *3*(5), 1–17.

Kołodziejczak-radzimska, A., & Jesionowski, T. (2014). *Zinc Oxide—From Synthesis to Application: A Review*. 2833–2881.

Kulkarni, S. S. (2015). *Optical and Structural Properties of Zinc Oxide Nanoparticles*. *2*(1), 14–18.

Liu, W. (2006). *Nanoparticles and Their Biological and Environmental Applications*. *102*(1), 1–7.

Mahboubi, M. (2019). Zingiber officinale Rosc. essential oil, a review on its composition and

bioactivity. *Clinical Phytoscience*, *5*(1), 1–12.

Manju, Jain, M., Madas, S., Vashishtha, P., Rajput, P., Gupta, G., Kahaly, M. U., Özdoğan, K., Vij, A., & Thakur, A. (2020). Oxygen vacancies induced photoluminescence in SrZnO 2 nanophosphors probed by theoretical and experimental analysis. *Scientific Reports*, *10*(1), 1–10.

Mofid, H., Seyed Sadjadi, M., Hossaini Sadr, M., Banaei, A., & Farhadyar, N. (2020). Green synthesis of zinc oxide nanoparticles using Aloe Vera plant for investigation of antibacterial properties. *Advances in Nanochemistry*, *2*(1), 31–35.

Muthuchamy, N., Atchudan, R., Nesakumar, T., & Immanuel, J. (2018). High-performance glucose biosensor based on green synthesized zinc oxide nanoparticle embedded nitrogen-doped carbon sheet. *Journal of Electroanalytical Chemistry*, *816*(January), 195–204.

Naseer, M., Aslam, U., Khalid, B., & Chen, B. (2020). Green route to synthesize Zinc Oxide Nanoparticles using leaf extracts of Cassia fistula and Melia azadarach and their antibacterial potential. *Scientific Reports*, *10*(1), 1–10.

Philip, D. (2009). *Spectrochimica Acta Part A : Molecular and Biomolecular Spectroscopy Honey mediated green synthesis of gold nanoparticles*. *73*, 650–653.

Poole, C. P., & Owens, F. J. (2003.). *Introduction to Nanotechnology*: A *John Wiley 81Sons, Inc., publication 66, 620*.

Pournaderi, P. S., Hejazi, S. H., & Yaghmaei, P. (2017). Comparing the therapeutic effects of 6-gingerol and hydro-alcoholic extract of ginger on polycystic ovary syndrome in Wistar rat. *Advanced Herbal Medicine*, *3*(2), 33–41.

Rajiv, P., Rajeshwari, S., & Venckatesh, R. (2013). Spectrochimica Acta Part A : Molecular and Biomolecular Spectroscopy Bio-Fabrication of zinc oxide nanoparticles using leaf extract of Parthenium hysterophorus L . and its size-dependent antifungal activity against plant fungal pathogens. *Spectrochimica Acta Part A: Molecular and Biomolecular Spectroscopy*, *112*, 384–387.

Salam, H. A., & Sivaraj, R. (2014). Green synthesis and characterization of zinc oxide Nanoparticles from *Ocimum basilicum* L. var. *purpurascens* Benth.-*LAMIACEAE* leaf extract: *Materials Letters, 11, 167-577*.

Shanmugapriya, J., Monisha, P., Nandhini, A., & Praveena, K. (2019). *Synthesis of Zinc Oxide Nano Particles from Aloe Barbadensis for Medical Application*. *7*(02), 1–10.

Sharma, D. K., & Singh, K. S. (2009). *in Direct and Indirect Band Gap Crystals*. *23*(23), 2783–2789.

Shukla, R., Nune, S. K., Chanda, N., Katti, K., Mekapothula, S., Kulkarni, R. R., Welshons, W. V, Kannan, R., & Katti, K. V. (2008). *Green chemistry Soybeans as a Phytochemical Reservoir for the Production and Stabilization of Biocompatible Gold Nanoparticles*. 1425–1436.

Singh, U. P., Prithiviraj, B., Sarma, B. K., Mandavi Singh, & Ray, A. B. (2001). Role of garlic (Allium sativum L.) in human and plant diseases. *Indian Journal of Experimental Biology*, *39*(4), 310–322.

Singhal, G., & Bhavesh, R. (2011). *Biosynthesis of silver nanoparticles using Ocimum sanctum (Tulsi) leaf extract and screening its antimicrobial activity*. 2981–2988.

Smuleac, V., Varma, R., Sikdar, S., & Bhattacharyya, D. (2011). Green synthesis of Fe and Fe / Pd bimetallic nanoparticles in membranes for reductive degradation of chlorinated organics. *Journal of Membrane Science*, *379*(1–2), 131–137.

Song, J., Zhou, J., & Wang, Z. L. (2006). *Piezoelectric and Semiconducting Coupled Power Generating Process of a Single ZnO Belt / Wire . A Technology for Harvesting Electricity from the Environment*.

Sun, L., & Hong, B. H. (2021). Chemical vapour deposition. *Nature Reviews Methods Primers*, *0123456789*.

Vidya, C., Hiremath, S., Chandraprabha, M. N., Antonyraj, M. A. L., & Venu, I. (2013). *Green synthesis of ZnO nanoparticles by Calotropis Gigantea*. *Ncwse*, 2012–2014.

Von White, G., Kerscher, P., Brown, R. M., Morella, J. D., McAllister, W., Dean, D., & Kitchens, C. L. (2012). Green synthesis of robust, biocompatible silver nanoparticles using garlic extract. *Journal of Nanomaterials*, *2012*.

Wang, X., Ding, Y., Summers, C. J., & Wang, Z. L. (2004). *Large-Scale Synthesis of Six-Nanometer-Wide ZnO Nanobelts*. *0245*, 8773–8777.

Yan, K. A. I., Fu, L. E. I., Peng, H., & Liu, Z. (2013). *Designed CVD Growth of Graphene via Process Engineering*. *XXX*(Xx).

Yuvakkumar, R., Suresh, J., Nathanael, A. J., Sundrarajan, M., & Hong, S. I. (2014). Novel green synthetic strategy to prepare ZnO nanocrystals using rambutan (*Nephelium lappaceum L.*) peel extract and its antibacterial applications. *Materials Science & Engineering C, 31, 305-764*.